Chapter 4

Metal Hydride-Based Materials as Negative Electrode for All-Solid-State Lithium-Ion Batteries

Liang Zeng, Koji Kawahito and Takayuki Ichikawa

Additional information is available at the end of the chapter

http://dx.doi.org/10.5772/62866

Abstract

The recently developed metal hydride (MH)-based material is considered to be a potential negative material for lithium-ion batteries, owing to its high theoretical Li storage capacity, relatively low volume expansion, and suitable working potential with very small polarization. However, it suffers from the slow kinetics, poor reversibility, and unfavourable cyclability in conventional organic liquid electrolyte systems, which enormously limit its practical application. In this chapter, we describe an all-solid-state battery system consisting of MH working electrode, $LiBH_4$ solid electrolyte, and Li metal counter electrode. The electrochemical properties of MgH_2 and TiH_2 composites are investigated, which showed much better performances using $LiBH_4$ as solid-state electrolyte than using conventional organic liquid electrolyte.

Keywords: Metal hydride, battery, solid state, conversion electrode, lithium-ion

1. Introduction

Currently, lithium-ion batteries (LIBs) with zero emission are considered to be the most important energy carrier in our daily life, which are absolutely imperative devices to power mobile phones, laptops, electric vehicles (EVs), and so on [1, 2]. Developing high-capacity materials for LIBs is necessary to satisfy the continuously rising need for energy. In the past tens of years, graphite is always used as negative electrode for commercial LIBs with an insufficient specific capacity (370 Ah kg^{-1}, 840 Ah L^{-1}) [3]. To overcome these restrictions, new concepts for the negative electrode must be developed. In other words, seeking suitable high-performance anode materials is essential and urgent.

In order to develop LIBs with high energy density, the conversion-type electrode materials had been intensively studied in recent years owing to their high Li storage capacity [2, 4]. In 2008, metal hydride (MH) was firstly reported as negative electrode for this purpose [5]. Compared to other conversion-type electrode materials, MH exhibits not only high theoretical Li storage capacities, but also relatively low volume expansions and suitable working potentials with very small polarization between charge and discharge [6]. The Li^+ insertion/extraction reactions for MHs can be written by the following hydride conversion reaction:

$$MH_x + x\,Li^+ + x\,e^- \leftrightarrow M + x\,LiH \quad (1)$$

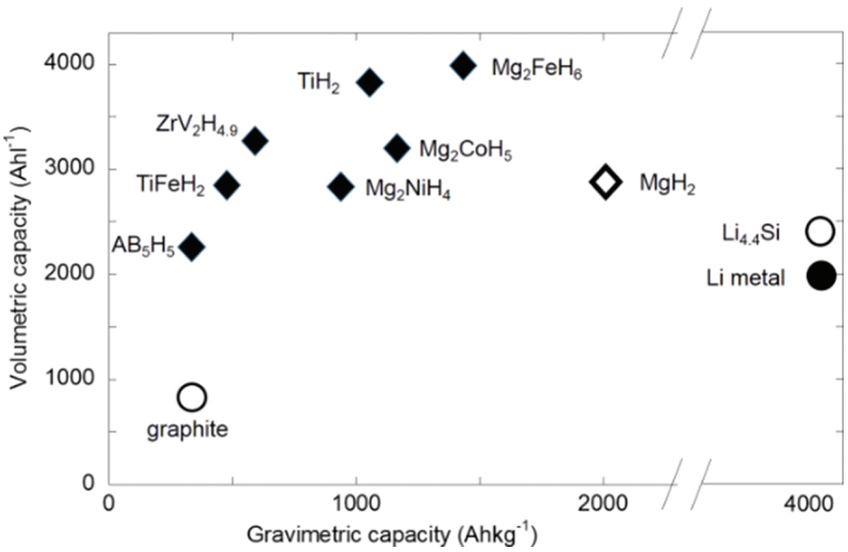

Figure 1. Theoretical gravimetric and volumetric capacities of metals and complex hydrides compared with those of graphite and other materials for negative electrodes. Reproduced from Ref. [6].

The theoretical gravimetric and volumetric capacities of some potential MHs as negative electrode for LIBs are shown in **Figure 1**. It can be seen that the capacities of all hydrides presented in this figure are larger than that of graphite. MgH_2 possesses the highest gravimetric capacity of 2038 Ah kg^{-1}, while Mg_2FeH_6 possesses the highest volumetric capacity of 3995 Ah L^{-1}. These large capacities lead MHs to a good candidate material for negative electrodes in LIBs for stationary as well as mobile applications for which the volumetric capacity plays a key role [6].

2. Metal hydride electrodes working in conventional organic liquid electrolyte systems

Among all of the MHs, MgH_2 is considered as the most promising candidate owing to its high theoretical Li storage capacity of 2038 mAh g^{-1}, a suitable working potential of around 0.5 V

http://dx.doi.org/10.5772/62866

(vs Li^+/Li), a relatively small volume change of 83%, and so on [5, 7]. The Li^+ insertion/extraction reaction of MgH_2 can be written by the following hydride conversion:

$$MgH_2 + 2\,Li^+ + 2\,e^- \leftrightarrow Mg + 2\,LiH \tag{2}$$

Further lithiation results in Li–Mg alloying reaction, which is partially irreversible.

$$Mg + x\,Li^+ + x\,e^- \leftrightarrow MgLi_x \tag{3}$$

For instance, the MgH_2 electrode working in 1 M $LiPF_6$ (DMC:EC=1:1) showed a reversible capacity of 1480 mAh g^{-1} in the first cycle; however, the capacity fades rapidly and reduces to less than 200 mAh g^{-1} after only 10 cycles. Sustained capacities could be achieved only by using a special copper foam current collector for particle confinement and limiting the reaction to 520 mAh g^{-1} [5]. A more recent report shows that a reversible capacity of about 500 mAh g^{-1} can be obtained after 20 discharge–charge cycles at a rate of 0.05 C with using nanoconfinement technique for MgH_2, but the coulombic efficiency of the first cycle is less than 50% [8].

After the discovery of MH as negative material for LIBs by Oumellal et al, some other groups followed their work and extended the research to many other hydrides, that is, TiH_2, TiNiH, Mg_2FeH_6, AlH_3, $LiAlH_4$, $NaAlH_4$, and so on [6, 8–24]. The electrochemical performances of these materials are summarized in **Table 1**.

Sample	Theoretical capacity (mAh g^{-1})	Reversible capacity of 1st cycle (mAh g^{-1})	Current density (C)	Cycling performance	Composition of electrode	Voltage range (V vs Li/Li^+)	Reference
MgH_2	2038	1480	1/20	520 mAh g^{-1} after 50 cycles[*1]	MgH_2:Carbon SP = 85:15	0.15–3.0	[5]
MgH_2	2038	1000	1/20	Less than 50 mAh g^{-1} after 10 cycles	MgH_2:PVdF:Super P carbon = 7:1:2	0.2–2.5	[9]
MgH_2	2038	1900	1/20	542 mAh g^{-1} after 40 cycles	MgH_2:CMC-f:$C_{7,460}$ carbon = 1:1:1	0.005–3.0	[10]
TiH_2	1074	1072[*2]	1/200	N/A	TiH_2:$C_{150,480}$ carbon = 10:1	0.005–3.0	[11]
TiNiH	248	251[*3]	1/10	N/A	TiNiH:Super P carbon = 10:1	0.005–3.0	[12]
Mg_2FeH_6	1454	1577[*4]	1/60	N/A	Mg_2FeH_6:$C_{150,480}$ carbon = 10:1	0.005–3.0	[13]
Mg_2CoH_5	1189	1300[*5]	1/50	N/A	Mg_2CoH_5:$C_{150,480}$ carbon = 10:1	0.005–3.0	[13]

Sample	Theoretical capacity (mAh g^{-1})	Reversible capacity of 1st cycle (mAh g^{-1})	Current density (C)	Cycling performance	Composition of electrode	Voltage range (V vs Li/Li^+)	Reference
Mg_2NiH_4	962	866*6	1/40	N/A	Mg_2NiH_4:$C_{150,480}$ carbon = 10:1	0.005–3.0	[13]
MgH_2	2038	950	1/20	500 mAh g^{-1} after 20 cycles	50MgH_2@HSAG-500:SP carbon = 80:20	0.005–3.0	[8]
$LiAlH_4$	2119	189	1/20	N/A	$LiAlH_4$:PVdF:Super P carbon = 5:2:3	0.01–2.5	[14]
Li_3AlH_6	1493	198	1/20	N/A	Li_3AlH_6:PVdF:Super P carbon = 5:2:3	0.01–2.5	[14]
TiH_2/C	1074	160	1/100	N/A	TiH_2:PVdF:Super P carbon = 5:2:3	0.01–2.0	[15]
$Mg_{0.7}Ti_{0.3}H_2$	1748	1540	1/20	530 mAh g^{-1} after 7 cycles	MgH_2:TiH_2:$C_{t,x}$ = 7:3:1	0.005–3.0	[16]
AlH_3	2678	1100	1/30	393 mAh g^{-1} after 10cycles	AlH_3:AB:CMC-f = 1:1:1	0.005–3.0	[17]
$NaAlH_4$	1984	770	1/30	250 mAh g^{-1} after 10 cycles	$NaAlH_4$:AB:CMC-f = 1:1:1	0.005–3.0	[17]

*1 Cycled using a pressed copper foam current collector.
*2*3*4*5*6 Only discharge capacity was shown.

Table 1. Electrochemical performance of metal hydrides in conventional organic liquid electrolyte (1M $LiPF_6$ (DMC:EC=1:1).

In spite of numerous advantages of MH mentioned above, the research on MH as negative electrode materials did not get enough attention since it suffers from the slow kinetics, poor reversibility, and unfavourable cyclability in conventional organic liquid electrolyte systems, which enormously limits its practical application.

3. MgH_2 composite electrode working with $LiBH_4$ solid-state electrolyte

From the above results, it can be inferred that the conventional organic liquid electrolyte systems might not be suitable for MH electrodes, thus an idea of using solid-state Li-ion conductor as electrolyte had come out.

There are many types of solid-state Li-ion conductors, including LISICON-type, Garnet-type, Perovskite-type, NASICON-type lithium-ion conductors, and glassy and glass-ceramic systems made of oxides and sulphides [25, 26]. When seeking a suitable medium to achieve a reversible conversion reaction by MH shown by Eq. (2), the Li^+ conductivity is one side to be considered, and another important factor is the H^- conductivity. As we know, the MgH_2–

http://dx.doi.org/10.5772/62866

$LiBH_4$ composite is a well-known material in hydrogen storage research field. In this system, the mobility of H^- in MgH_2 can be strongly enhanced by $LiBH_4$, due to a superior hydrogen exchange effect between MgH_2 and $LiBH_4$ [27]. That is to say, this effect may lead to a significant improvement of H^- conductivity when using this material as negative electrode for LIB. In the meantime, it was reported that $LiBH_4$ showed remarkable high Li-ion conductivity to the order of 10^{-3} S cm^{-1} at its HT phase (>115°C) with a very stable operating window between 0 and 5 V vs Li^+/Li, which can be used as solid-state electrolyte for LIBs [26, 28–30]. Considering the above two effects, when using MgH_2–$LiBH_4$ as negative electrode and $LiBH_4$ as solid-state electrolyte, the hydride conversion reaction of Eq. (2) could be dramatically accelerated, which may lead to much better battery performance for reversibility and cyclability.

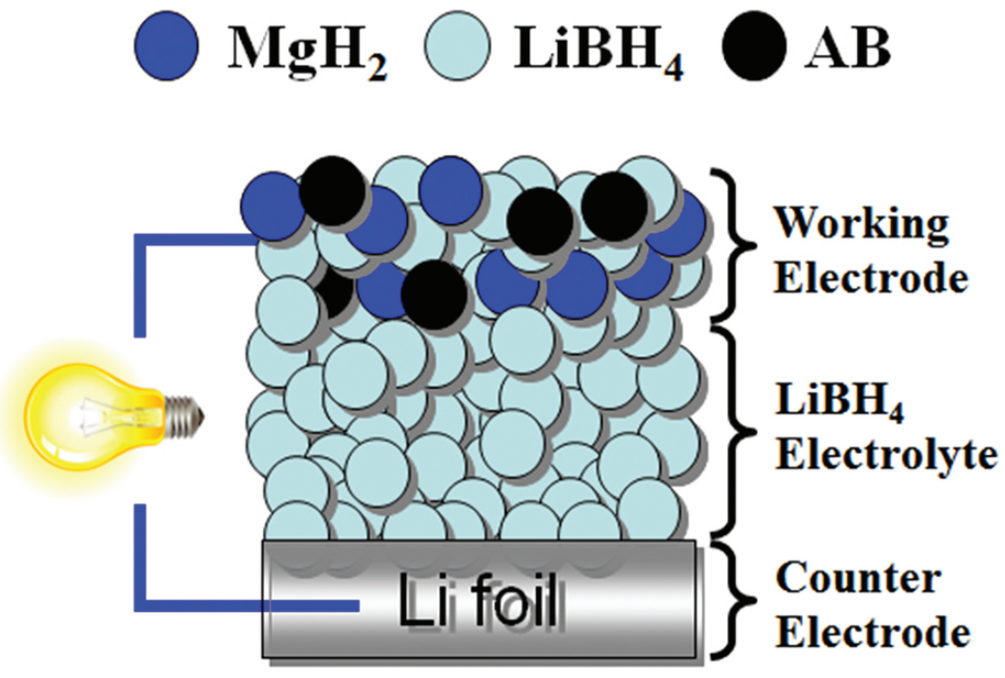

Figure 2. The schematic illustration of the MgH_2–$LiBH_4$|$LiBH_4$|Li all-solid-state battery.

In this part, a battery cell constructed of MgH_2–$LiBH_4$|$LiBH_4$|Li (illustrated in **Figure 2**) had been fabricated for electrochemical tests. 1 mol% Nb_2O_5-doped MgH_2 (named c-MgH_2 hereafter) was also used in this study for comparison, which had been proved to have positive effect in battery performance [20, 21, 23]. The working electrode was prepared by simply ball-milling MgH_2/c-MgH_2, $LiBH_4$, and conductive carbon (acetylene black) with no further optimization. The thermal stability of MgH_2–$LiBH_4$ composite was measured by thermogravimetry with differential thermal analysis (TG–DTA), which shows a weight loss of less than 1 wt% in the temperature of RT–275°C (**Figure 3**). To obtain the fast Li^+ conduction from $LiBH_4$, all electrochemical measurements in this study were conducted at 120°C. The electrode evolution upon discharge–charge process at different stages was investigated by means of powder X-ray diffraction (XRD).

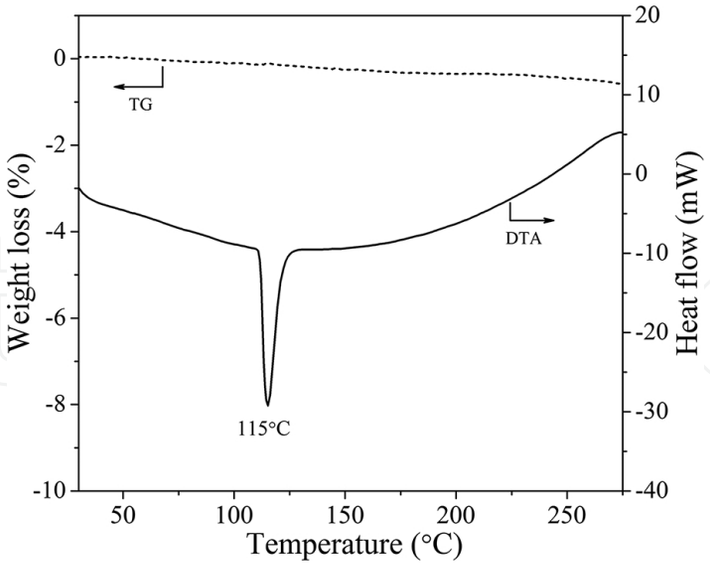

Figure 3. The TG–DTA result of the MgH_2–$LiBH_4$ composite heating up to 275°C.

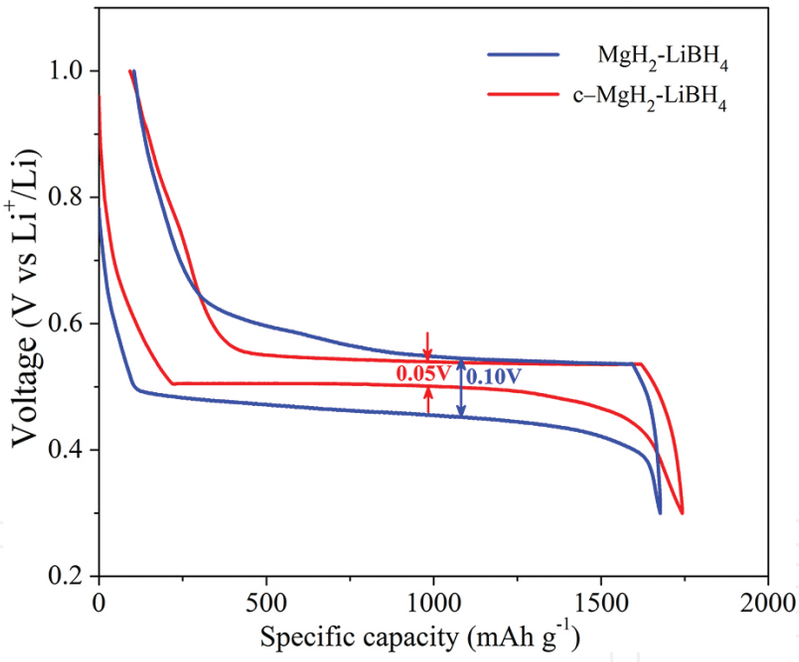

Figure 4. The first galvanostatic discharge–charge curves for MgH_2–$LiBH_4$ and c-MgH_2–$LiBH_4$ composite electrodes in the voltage range of 0.3–1.0 V at a current density of 100 mA g^{-1} at 120°C, respectively.

Figure 4 shows the first galvanostatic discharge–charge curves for MgH_2–$LiBH_4$ and c-MgH_2–$LiBH_4$ composite electrodes using $LiBH_4$ as solid-state electrolyte in the voltage range of 0.3–1.0 V vs Li^+/Li at a current density of 100 mA g^{-1}. It can be seen that on the discharge curve (Li^+ incorporation into MgH_2), the potential gradually dropped to near 0.5 V, followed by showing a long flat plateau for c-MgH_2 electrode and a slope for MgH_2 electrode, corresponding to the hydride conversion reaction shown by Eq. (2). The discharge process was cut at 0.3 V to avoid

http://dx.doi.org/10.5772/62866

the Li–Mg alloying reaction: $Mg + x\ Li^+ + x\ e^- \leftrightarrow MgLi_x$, which is a partial irreversible reaction and would weaken the cyclability of MgH_2. On the charge curve (Li^+ extraction), a plateau slightly above 0.5 V was observed for both samples. The polarization between Li insertion and extraction was 0.1 V for MgH_2 electrode and 0.05 V for c-MgH_2 electrode, which are much smaller than that of the MgH_2 electrodes working with organic liquid-based electrolyte in some previous reports [5, 9]. Such a small polarization could be owing to the high working temperature of 120°C, which brings better kinetic properties to the reaction. The initial reversible capacity and coulombic efficiency were 1650 mAh g^{-1} and 94.7% for c-MgH_2 electrode and 1572 mAh g^{-1} and 93.7% for MgH_2 electrode. The above results indicated that the existence of $LiBH_4$ significantly promoted the hydride conversion reaction due to its dual effects on Li^+ conductivity and H^- conductivity. In addition, the Nb_2O_5 doping to MgH_2 further improves the reaction kinetics, resulting in better reversibility and higher initial coulombic efficiency.

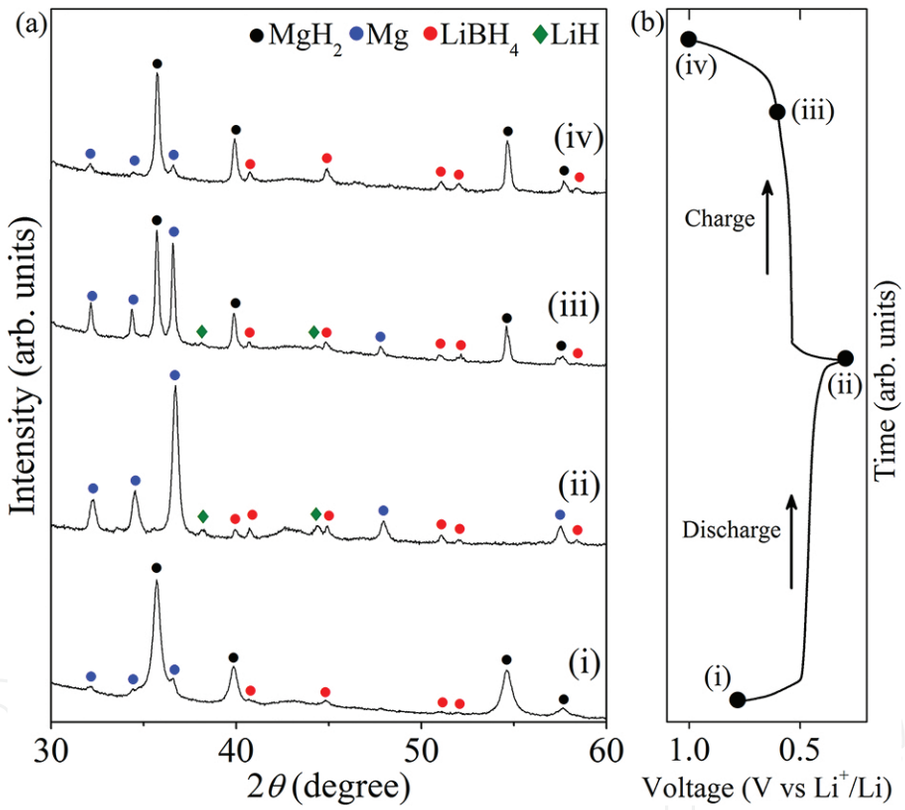

Figure 5. Ex situ XRD patterns of MgH_2–$LiBH_4$ composite electrode evolution upon the first electrochemical discharge–charge process at different stages.

The ex situ XRD measurement had been carried out at different stages upon the initial discharge–charge process shown by **Figure 5**. The $LiBH_4$ phase appeared in all the stages since it was included in the working electrode. At open circuit voltage stage (i), a small amount of Mg phase was detected in the XRD pattern as an impurity, which came from the as-received commercial MgH_2 sample. As Li reacted with MgH_2, the LiH and Mg peaks appeared while MgH_2 peaks disappeared at 0.3 V (ii), indicating the hydride conversion reaction shown by

Eq. (2) had occurred. When recharging the same battery cell, clear MgH_2 peaks reappeared with weakened LiH and Mg peaks at the intermediate stage (iii). Finally, the LiH phase totally disappeared with a very small amount of Mg at 1.0 V (iv), which is equivalent to stage (i). The above results verified the good reversibility of the hydride conversion reaction. Interestingly, a new phase of $Mg(BH_4)_2$ was found (**Figure 6**) when further charging the battery cell to 2.0 V, which implies a $Mg(BH_4)_2$ generation reaction might have occurred between 1.0 and 2.0 V shown by Eq. (4).

$$Mg + 2\ LiBH_4 \rightarrow Mg(BH_4)_2 + 2\ Li^+ + 2\ e^- \quad (4)$$

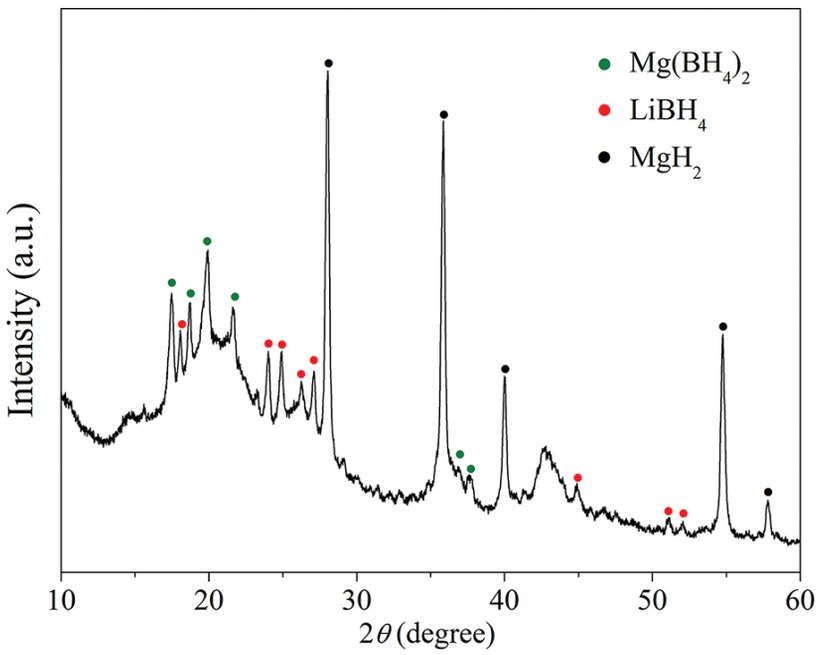

Figure 6. The XRD result of MgH_2–$LiBH_4$ composite electrode charged to 2.0 V.

To avoid this undesirable reaction, the galvanostatic discharge–charge cycling tests were performed between 0.3 and 1.0 V at a current density of 800 mA g^{-1} as shown in **Figure 7**. It shows that the MgH_2–$LiBH_4$ electrode delivered a highly reversible capacity of 1488 mAh g^{-1} in the first cycle; however, only 270 mAh g^{-1} remained after 93 cycles. In the meantime, a reversible capacity of 1586 mAh g^{-1} is shown in the first cycle for the Nb_2O_5-doped electrode, which retained at 700 mAh g^{-1} after cycling for 100 times. This result suggests the cyclability of the MgH_2–$LiBH_4$ electrode is also improved by the Nb_2O_5-doping effect. The galvanostatic discharge–charge curves of Nb_2O_5-doped electrode are shown by **Figure 8**. It can be observed that the plateau voltage of the discharge and charge profiles almost has no changes during 100 cycles with coulombic efficiency over 99.5%, which indicated that the working electrode operated properly between 0.3 and 1.0 V, namely, there was no side reaction during the

http://dx.doi.org/10.5772/62866

discharge–charge cycles. Moreover, the suitable Li insertion/extraction voltage of around 0.5 V (vs Li^+/Li) and the small polarization are particularly remarkable, making it a promising candidate as negative electrode material for LIBs.

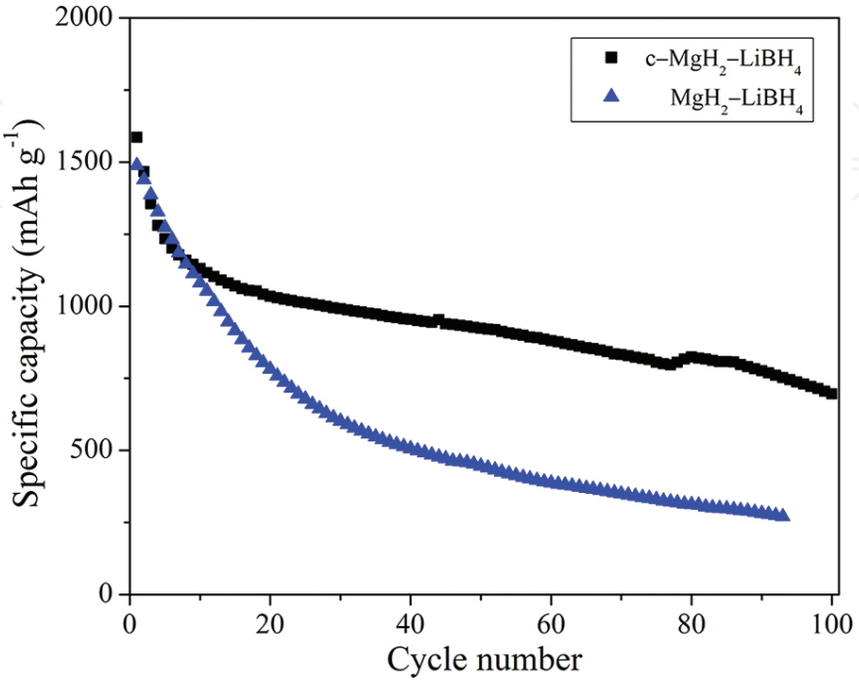

Figure 7. Cycling performances of MgH_2–$LiBH_4$ and c-MgH_2–$LiBH_4$ composite electrodes in the voltage range of 0.3–1.0 V at a current density of 800 mA g^{-1} at 120°C.

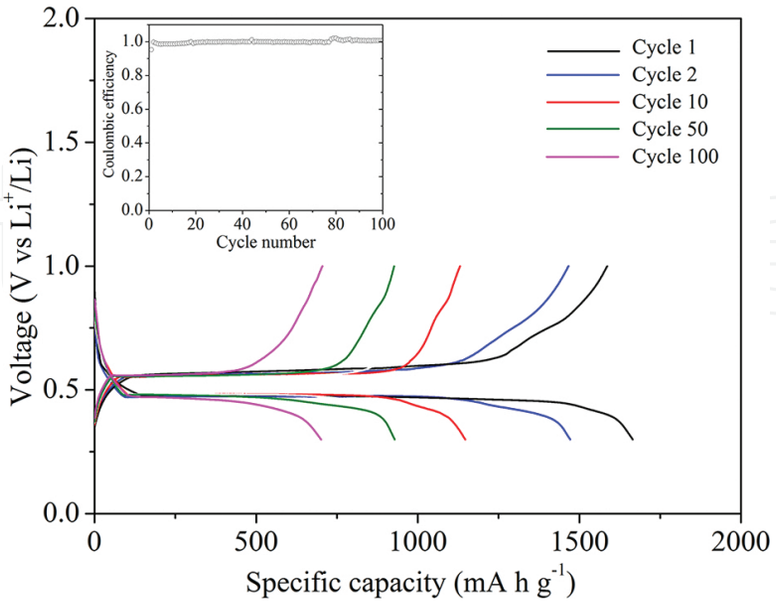

Figure 8. Galvanostatic discharge–charge curves for c-MgH_2–$LiBH_4$ composite electrode in the voltage range of 0.3–1.0 V at a current density of 800 mA g^{-1} at 120°C. Inset shows the coulombic efficiency for 100 cycles.

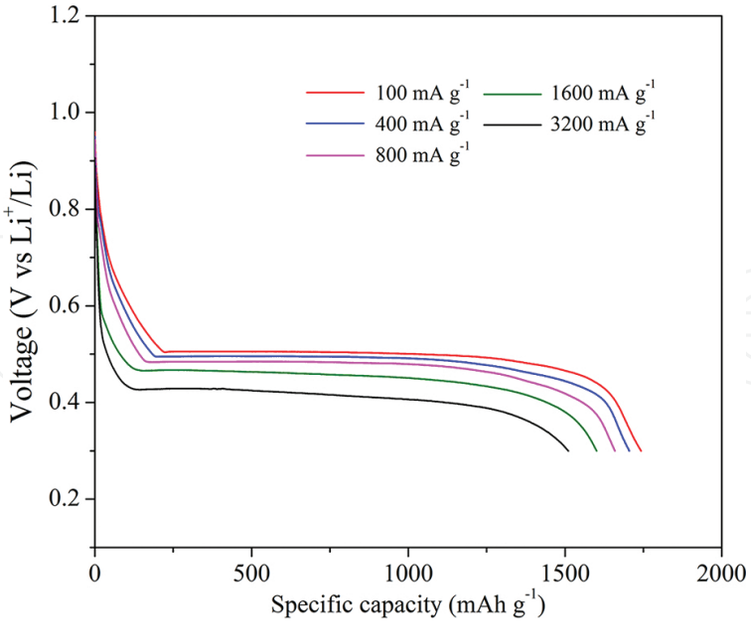

Figure 9. Rate performance of c-MgH_2–$LiBH_4$ composite electrodes at the current densities of 100–3200 mA g^{-1} at 120°C, respectively.

The rate capability of the Nb_2O_5-doped electrode (c-MgH_2–$LiBH_4$) was also investigated as shown by **Figure 9**. It can be seen that the discharge capacity was 1510, 1600, 1659, 1704, and 1742 mAh g^{-1} at the current density of 3200, 1600, 800, 400, and 100 mA g^{-1}, respectively, indicating that this sample possessed excellent rate capability. The fast kinetics of this material could be ascribed to rapid Li^+ and H^- diffusion in the working electrode and on the interface between electrode and electrolyte. It is worth noting that the plateau voltage gradually decreased along with increase in the current density, which was caused by the insufficiency of electrical conductivity at high discharging rate. As we know, the electrical conductivity of electrode material can be remarkably improved via surface modification technique, for example, carbon coating [31], which can be also applied in this system for future working direction in order to obtain better high rate performance.

4. TiH_2 electrode working with $LiBH_4$ solid-state electrolyte

Another promising candidate of MHs as negative electrode is titanium hydride (TiH_2), which has a theoretical capacity of 1074 mAh g^{-1} with a low working potential of 0.163 V vs Li^+/Li by the following reaction:

$$TiH_2 + 2\ Li^+ + 2\ e^- \leftrightarrow Ti + 2\ LiH \tag{5}$$

In the viewpoint of making high-power battery, TiH_2 is preferable to MgH_2 as negative electrode since its theoretical working potential is much lower than MgH_2, which leads to a

http://dx.doi.org/10.5772/62866

higher voltage for a full battery cell. The electrochemical Li insertion/extraction mechanism of TiH_2 was reported by Oumellal et al. [11]. However, the cyclic properties have not been reported yet due to the poor reversibility in conventional organic liquid-based electrolyte.

In this part, we had prepared the TiH_2–$LiBH_4$ composite as the negative electrode together with $LiBH_4$ as the solid-state electrolyte for an all-solid-state battery cell, in order to obtain good cyclic performance for TiH_2. This system is similar to the above content for MgH_2 electrode, which shows favourable electrochemical performances. The phase evolution of TiH_2 electrode upon charge–discharge in the solid-state cell, cyclic properties, and rate performance are investigated.

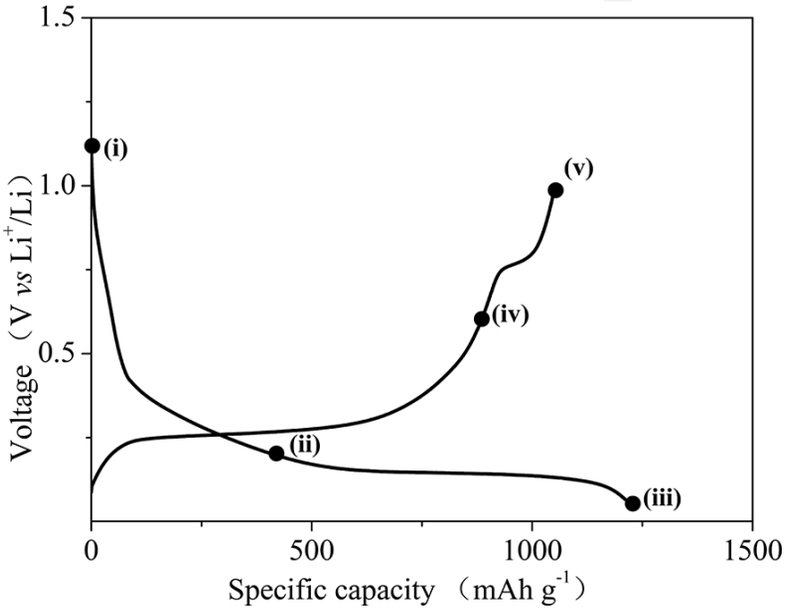

Figure 10. Initial galvanostatic charge–discharge curve for TiH_2–$LiBH_4$ electrode in the voltage range of 2.0–0.05 V at a current density of 400 mAh g^{-1} at 120°C.

Figure 10 shows the initial charge–discharge curves of the TiH_2 electrode between 1.0 and 0.05 V using $LiBH_4$ solid electrolyte under the current density of 400 mA g^{-1} at 120°C. The Li insertion curve shows slope and plateau regions: slope region (0.4–0.15 V) and plateau region (0.15 V). From some previously reported results [11], it was considered that the slope region indicated fcc-TiH_2 reacted with lithium to form LiH and partially transformed into a distorted orthorhombic phase fco-TiH_{2-x}, and slope region indicated that both of fcc-TiH_2 and fco-TiH_{2-x} react with lithium to form Ti and LiH ($TiH_2 + 2Li^+ + 2e^- \rightarrow Ti + 2LiH$). Unlike the case of MgH_2, no plateau could be observed below 0.15V, indicating that Ti did not electrochemically react with Li to form Li–Ti alloy. During the initial Li insertion, the capacity of 1225 mAh g^{-1} was obtained, while the theoretical capacity was 1074 mAh g^{-1}. This overcapacity could be due to the existence of acetylene black in the electrode, which contributes on the Li storage capacity as an anode.

On the Li extraction curve, the plateau corresponding to de-lithiation process of TiH_2 conversion reaction was observed at higher voltages than 0.15 V, indicating the higher polarization

of electrode compared with the case of MgH_2 system [23]. Furthermore, a short plateau at 0.75 V was observed and the whole Li extraction curve showed 1052 mAh g^{-1} corresponding to 86% coulombic efficiency.

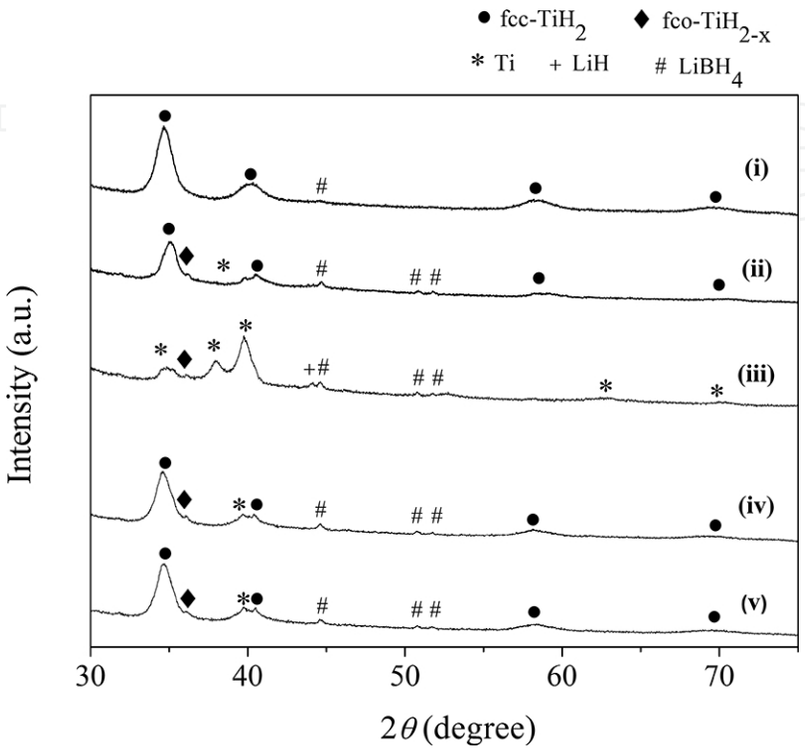

Figure 11. Ex situ XRD patterns of TiH_2–$LiBH_4$ at the various states of charge.

In order to identify the electrochemical reaction, ex situ XRD measurements were performed at the different states of charges as shown in **Figure 11**. It is noteworthy that all the profiles shown in **Figure 11** contain peaks corresponding to $LiBH_4$, which should always be included in the electrodes. At the initial state (i), the broad peaks corresponding to TiH_2 were observed due to the ball-milling effect. After the Li insertion (ii), the broad peaks slightly shifted to higher angle, indicating that the TiH_2 structure should be slightly shrunk due to partial extraction of hydrogen. And a small peak corresponding to fco-TiH_{2-x} and Ti were observed. With further lithiation (iii), it was clearly observed that the TiH_2 changed to Ti and LiH. For the Li extraction process, H atoms were transferred from LiH to Ti. Then, as shown in **Figure 10** (iv, v), peaks corresponding to TiH_2 reappeared, then the Ti peak was strongly reduced. These facts indicate that TiH_2 electrode reveals high electrochemical performance by using the $LiBH_4$ solid-state electrolyte. The combination of hydride and borohydride for anode and electrolyte, respectively, could lead to a better performance.

Unfortunately, the reaction at 0.75 V as shown in **Figure 10** was not clarified, yet even though we have performed the XRD measurement at various states of charge. As one of the possible reasons, it could be caused by the Li extraction process from acetylene black, which cannot be detected by XRD due to its amorphous feature.

http://dx.doi.org/10.5772/62866

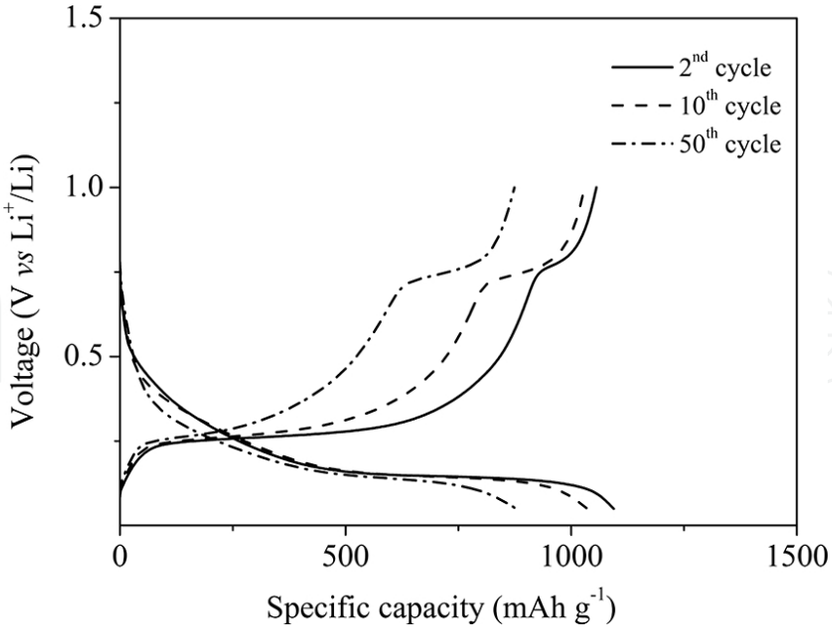

Figure 12. Cyclic performance of the TiH_2–$LiBH_4$ composite electrode in the voltage range of 1.0–0.05 V at a current density of 400 mA g^{-1} at 120°C.

Figure 12 shows the cyclic performance of TiH_2–$LiBH_4$ composite electrode in the voltage range of 1.0–0.05 V at a current density of 400 mA g^{-1} at 120°C. Almost the same profile as the initial cycle was observed in later cycles. The Li insertion capacities of the 2nd, 10th, and 50th cycles were 1094, 1035, and 878 mAh g^{-1}, respectively, which corresponding to a capacity retention of about 80% for 50 charge–discharge cycles. This result revealed for the first time that the

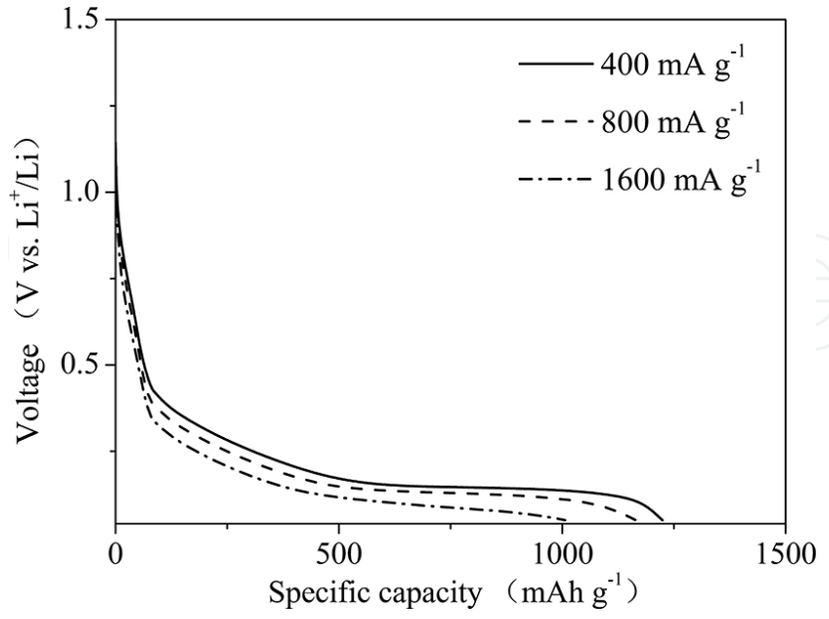

Figure 13. Rate capability of the TiH_2–$LiBH_4$ composite electrode at a current density of 400, 800, and 1600 mA g^{-1} at 120°C.

charge–discharge process of TiH_2 electrode is recyclable, which makes it a promising candidate for LIBs.

The rate capability of the TiH_2 composite electrode was also investigated as shown in **Figure 13**. All the discharge profiles in this figure were created by the initial discharge cycle of independent cells at different current densities of 400, 800, and 1600 mA g^{-1}, which are corresponding to about 1/3 C, 2/3 C, and 4/3 C, respectively. It can be seen that discharge capacity was 1225, 1165, and 1007 mAh g^{-1} at the current density of 400, 800, and 1600 mA g^{-1}, respectively, indicating a very good rate capability of TiH_2 electrode in this system. For comparison, the charge–discharge for TiH_2 in a conventional organic electrolyte could be performed only at 10 mA g^{-1} [6]. Like in the MgH_2 system, the fast kinetics of TiH_2 could also be ascribed to rapid Li^+ and H^- diffusion in the electrode material and on the electrode–electrolyte interface at a high working temperature of 120°C.

5. Summary

In summary, we have demonstrated an all-solid-state battery system consisting of MH working electrode, $LiBH_4$ solid electrolyte, and Li metal counter electrode. The MgH_2–$LiBH_4$ and TiH_2–$LiBH_4$ composite electrodes showed much better performances using $LiBH_4$ as solid-state electrolyte than using conventional organic liquid electrolyte in some previous reports. $LiBH_4$ here acts as multifunctional ion conductor, promotes not only Li^+ but also H^- conductivity, resulting in much higher reversibility for the hydride conversion reaction. In addition, Nb_2O_5 doping shows significant improvement on cyclability of MgH_2. The suitable operating voltage, large reversible capacity, and the very small polarization are particularly remarkable to make MH a promising negative electrode material for all-solid-state LIBs. Besides, not only $LiBH_4$ but also a large number of hydride-based solid-state alternatives for example, $Li_m(BH_4)_nX$ (X = Cl, Br, I) [29, 32], $LiBH_4$–$LiNH_2$ [29, 33], and $LiAlH_4$/Li_3AlH_6 [34] can also be considered for this system. The working temperature can be altered while using these various substitutions, some of which even show high Li-ion conductivity at room temperature. This work shows a new direction to search for potential high-performance negative electrode materials for LIBs. The electrochemical performance of numerous MH-based materials will be investigated in a similar system as in this article in the future.

Author details

Liang Zeng[1], Koji Kawahito[2] and Takayuki Ichikawa[1,3*]

*Address all correspondence to: tichi@hiroshima-u.ac.jp

1 Institute for Advanced Materials Research, Hiroshima University, Japan

2 Graduate School of Advanced Sciences of Matter, Hiroshima University, Japan

3 Graduate School of Integrated Arts and Sciences, Hiroshima University, Japan

References

[1] Armand M, Tarascon JM. Building better batteries. Nature. 2008;451:652–657. DOI: 10.1038/451652a

[2] Bruce PG, Scrosati B, Tarascon JM. Nanomaterials for rechargeable lithium batteries. Angew. Chem. Int. Ed. 2008;47:2930–2946. DOI: 10.1002/anie.200702505

[3] Arico AS, Bruce P, Scrosati B, Tarascon JM, Van Schalkwijk W. Nanostructured materials for advanced energy conversion and storage devices. Nat. Mater. 2005;4:366–377. DOI: 10.1038/Nmat1368

[4] Reddy MV, Rao GVS, Chowdari BVR. Metal Oxides and Oxysalts as Anode Materials for Li Ion Batteries. Chem. Rev. 2013;113:5364–5457. DOI: 10.1021/Cr3001884

[5] Oumellal Y, Rougier A, Nazri GA, Tarascon JM, Aymard L. Metal hydrides for lithium-ion batteries. Nat. Mater. 2008;7:916–921. DOI: 10.1038/Nmat2288

[6] Aymard L, Oumellal Y, Bonnet JP. Metal hydrides: an innovative and challenging conversion reaction anode for lithium-ion batteries. Beilstein J. Nanotech. 2015;6:1821–1839. DOI: 10.3762/bjnano.6.186

[7] Oumellal Y, Rougier A, Tarascon JM, Aymard L. 2LiH+M (M = Mg, Ti): New concept of negative electrode for rechargeable lithium-ion batteries. J. Power Sources. 2009;192:698–702. DOI: 10.1016/j.jpowsour.2009.03.003

[8] Oumellal Y, Zlotea C, Bastide S, Cachet-Vivier C, Leonel E, Sengmany S, Leroy E, Aymard L, Bonnet JP, Latroche M. Bottom-up preparation of MgH2 nanoparticles with enhanced cycle life stability during electrochemical conversion in Li-ion batteries. Nanoscale. 2014;6:14459–14466. DOI: 10.1039/C4nr03444a

[9] Brutti S, Mulas G, Piciollo E, Panero S, Reale P. Magnesium hydride as a high capacity negative electrode for lithium ion batteries. J. Mater. Chem. 2012;22:14531–14537. DOI: 10.1039/C2jm31827j

[10] Zaidi W, Oumellal Y, Bonnet JP, Zhang J, Cuevas F, Latroche M, Bobet JL, Aymard L. Carboxymethylcellulose and carboxymethylcellulose-formate as binders in MgH2-carbon composites negative electrode for lithium-ion batteries. J. Power Sources. 2011;196:2854–2857. DOI: 10.1016/j.jpowsour.2010.11.048

[11] Oumellal Y, Zaidi W, Bonnet JP, Cuevas F, Latroche M, Zhang J, Bobet JL, Rougier A, Aymard L. Reactivity of TiH2 hydride with lithium ion: Evidence for a new conversion mechanism. Int. J. Hydrogen Energy. 2012;37:7831–7835. DOI: 10.1016/j.ijhydene.2012.01.107

[12] Bououdina M, Oumellal Y, Dupont L, Aymard L, Al-Gharni H, Al-Hajry A, Maark TA, De Sarkar A, Ahuja R, Deshpande MD, Qian Z, Rahane AB. Lithium storage in amorphous TiNi hydride: Electrode for rechargeable lithium-ion batteries. Mater. Chem. Phys. 2013;141:348–354. DOI: 10.1016/j.matchemphys.2013.05.021

[13] Zaidi W, Bonnet JP, Zhang J, Cuevas F, Latroche M, Couillaud S, Bobet JL, Sougrati MT, Jumas JC, Aymard L. Reactivity of complex hydrides Mg2FeH6, Mg2CoH5 and Mg2NiH4 with lithium ion: Far from equilibrium electrochemically driven conversion reactions. Int. J. Hydrogen Energy. 2013;38:4798–4808. DOI: 10.1016/j.ijhydene.2013.01.157

[14] Silvestri L, Forgia S, Farina L, Meggiolaro D, Panero S, La Barbera A, Brutti S, Reale P. Lithium Alanates as Negative Electrodes in Lithium-Ion Batteries. Chemelectrochem. 2015;2:877–886. DOI: 10.1002/celc.201402440

[15] Vitucci F, Paolone A, Brutti S, Munaò D, Silvestri L, Panero S, Reale P. H2 thermal desorption and hydride conversion reactions in Li cells of TiH2/C amorphous nanocomposites. J. Alloys Compd. 2015;645:S46–S50. DOI: 10.1016/j.jallcom.2015.01.232

[16] Huang L, Aymard L, Bonnet JP. MgH2-TiH2 mixture as an anode for lithium-ion batteries: synergic enhancement of the conversion electrode electrochemical performance. J. Mater. Chem. A. 2015;3:15091–15096. DOI: 10.1039/c5ta02545a

[17] Teprovich JA, Zhang JX, Colon-Mercado H, Cuevas F, Peters B, Greenway S, Zidan R, Latroche M. Li-Driven Electrochemical Conversion Reaction of AIH3, LiAIlH4, and NaAlH4. J. Phys. Chem. C. 2015;119:4666–4674. DOI: 10.1021/jp5129595

[18] Zhang JX, Zaidi W, Paul-Boncour V, Provost K, Michalowicz A, Cuevas F, Latroche M, Belin S, Bonnet JP, Aymard L. XAS investigations on nanocrystalline Mg2FeH6 used as a negative electrode of Li-ion batteries. J. Mater. Chem. A. 2013;1:4706–4717. DOI: 10.1039/C3ta01482g

[19] Meggiolaro D, Gigli G, Paolone A, Vitucci F, Brutti S. Incorporation of Lithium by MgH2: An Ab Initio Study. J. Phys. Chem. C. 2013;117:22467–22477. DOI: 10.1021/jp404993z

[20] Ikeda S, Ichikawa T, Kawahito K, Hirabayashi K, Miyaoka H, Kojima Y. Anode properties of magnesium hydride catalyzed with niobium oxide for an all solid-state lithium-ion battery. Chem. Commun. 2013;49:7174–7176. DOI: 10.1039/C3cc43987a

[21] Ikeda S, Ichikawa T, Goshome K, Yamaguchi S, Miyaoka H, Kojima Y. Anode properties of Al2O3-added MgH2 for all-solid-state lithium-ion batteries. J. Solid State Electr. 2015;19:3639–3644. DOI: 10.1007/s10008-015-2959-8

[22] Meggiolaro D, Gigli G, Paolone A, Reale P, Doublet ML, Brutti S. Origin of the Voltage Hysteresis of MgH2 Electrodes in Lithium Batteries. J. Phys. Chem. C. 2015;119:17044–17052. DOI: 10.1021/acs.jpcc.5b04615

[23] Zeng L, Kawahito K, Ikeda S, Ichikawa T, Miyaoka H, Kojima Y. Metal hydride-based materials towards high performance negative electrodes for all-solid-state lithium-ion batteries. Chem. Commun. 2015;51:9773–9776. DOI: 10.1039/c5cc02614h

[24] Kawahito K, Zeng L, Ichikawa T, Miyaoka H, Kojima Y. Electrochemical performance of titanium hydride for bulk-type all-solid-state lithium-ion batteries. Mater. Trans. DOI: 10.2320/matertrans.M2016024

[25] Jung YS, Oh DY, Nam YJ, Park KH. Issues and Challenges for Bulk-Type All-Solid-State Rechargeable Lithium Batteries using Sulfide Solid Electrolytes. Isr. J. Chem. 2015;55:472–485. DOI: 10.1002/ijch.201400112

[26] Takahashi K, Hattori K, Yamazaki T, Takada K, Matsuo M, Orimo S, Maekawa H, Takamura H. All-solid-state lithium battery with LiBH4 solid electrolyte. J. Power Sources. 2013;226:61–64. DOI: 10.1016/j.jpowsour.2012.10.079

[27] Zeng L, Miyaoka H, Ichikawa T, Kojima Y. Superior Hydrogen Exchange Effect in the MgH2-LiBH4 System. J. Phys. Chem. C. 2010;114:13132–13135. DOI: 10.1021/Jp1042443

[28] Matsuo M, Nakamori Y, Orimo S, Maekawa H, Takamura H. Lithium superionic conduction in lithium borohydride accompanied by structural transition. Appl. Phys. Lett. 2007;91:224103. DOI: 10.1063/1.2817934

[29] Matsuo M, Orimo S. Lithium Fast-Ionic Conduction in Complex Hydrides: Review and Prospects. Adv. Energy Mater. 2011;1:161–172. DOI: 10.1002/aenm.201000012

[30] Unemoto A, Matsuo M, Orimo S. Complex Hydrides for Electrochemical Energy Storage. Adv. Funct. Mater. 2014;24:2267–2279. DOI: 10.1002/adfm.201303147

[31] Li HQ, Zhou HS. Enhancing the performances of Li-ion batteries by carbon-coating: present and future. Chem. Commun. 2012;48:1201–1217. DOI: 10.1039/C1cc14764a

[32] Maekawa H, Matsuo M, Takamura H, Ando M, Noda Y, Karahashi T, Orimo SI. Halide-Stabilized LiBH4, a Room-Temperature Lithium Fast-Ion Conductor. J. Am. Chem. Soc. 2009;131:894–895. DOI: 10.1021/Ja807392k

[33] Matsuo M, Remhof A, Martelli P, Caputo R, Ernst M, Miura Y, Sato T, Oguchi H, Maekawa H, Takamura H, Borgschulte A, Zuttel A, Orimo S. Complex Hydrides with (BH4)(-) and (NH2)(-) Anions as New Lithium Fast-Ion Conductors. J. Am. Chem. Soc. 2009;131:16389–16391. DOI: 10.1021/Ja907249p

[34] Oguchi H, Matsuo M, Sato T, Takamura H, Maekawa H, Kuwano H, Orimo S. Lithium–ion conduction in complex hydrides LiAlH4 and Li3AlH6. J. Appl. Phys. 2010;107:096104. DOI: 10.1063/1.3356981

IntechOpen